Rapid Communication: Middle Pleistocene Transition as a Phenomenon of Orbitally Enabled Sensitivity to Initial Values

Mikhail Y. Verbitsky[1,2] and Anne Willem Omta[3]

[1]Gen5 Group, LLC, Newton, MA, USA
[2]UCLouvain, Earth and Life Institute, Louvain-la-Neuve, Belgium
[3]Department of Earth, Environmental, and Planetary Sciences, Case Western Reserve University, Cleveland, OH, USA
Correspondence: Mikhaïl Verbitsky (verbitskys@gmail.com)

Abstract. The Middle Pleistocene Transition (MPT), i.e., the "fast" transition from ~41- to ~100-kyr rhythmicity that occurred about 1 Myr ago, remains one of the most intriguing phenomena of the past climate. The cause of this period shift is generally thought to be a change within the Earth System, since the orbital insolation forcing does not change its pattern through the MPT. Using a dynamical model rooted in ocean chemistry, we advance several novel concepts here: (i) the MPT could be a dominant-period relaxation process that may be dependent on the initial state of the system, (ii) this sensitivity to the initial state is enabled by the orbital forcing, (iii) depending on the amplitude of the orbital forcing and initial values, the MPT could have been not just of the 40 – 80 kyr type, as we observe in the available data, but also of a 20 – 40, 40 – 120, or even 80 – 40 kyr type, (iv) when the orbital forcing of the global glaciation-climate model is accompanied by the alkalinity (CO_2) forcing containing a dominant-period shift from 41 kyr to 80 kyr, this ice-climate system produces a 40-to-100 kyr glacial rhythmicity transition resembling the MPT LR04 data, and (v) when the glaciation-climate model is forced by an alkalinity (CO_2) forcing containing a periodicity transition from 20 kyr to 42 kyr, a non-linear interplay of the orbital forcing and of ~40-kyr periods of the alkalinity forcing may produce glaciation periods of ~100 kyr that are also consistent with the LR04 data.

1. Introduction

Around 1 Myr ago, the dominant period of the glacial-interglacial cycles shifted from ~41 to ~100 kyr. The disambiguation of this change in glacial rhythmicity, i.e., the Middle Pleistocene Transition, or MPT hereafter, has been a challenge for the scientific community throughout the last few decades (e.g., Saltzman and Verbitsky, 1993; Clark and Pollard, 1998, Tziperman et al., 2006; Peacock al., 2006; Abe-Ouchi et al., 2013; Crucifix, 2013; Mitsui and Aihara, 2014; Paillard, 2015; Ashwin and Ditlevsen, 2015; Verbitsky et al., 2018; Willeit et al., 2019; Riechers et al., 2022; Shackleton et al, 2023; Carrillo et al, 2025; Scherrenberg et al., 2025; Pérez-Montero et al., 2025). Since the orbital insolation forcing does not change its pattern through the MPT, several proposed hypotheses included slow changes in governing parameters *internal to the Earth System.* These may define intensities of positive (e.g., variations in carbon dioxide concentration, Saltzman and Verbitsky, 1993) or negative (e.g., regolith erosion, Clark and Pollard, 1998) system feedbacks or a combination of positive and negative feedbacks (e.g., the interplay of ice-sheet vertical temperature advection and the geothermal heat flux, Verbitsky and Crucifix, 2021). The importance of the orbital forcing in generating the pre-MPT ~41 kyr cycles and post-MPT ~100 kyr cycles has widely been acknowledged. In particular, it has been suggested that orbital periods either directly drive these cycles (Raymo et al., 2006; Bintanja and Van de Wal, 2008; Tzedakis et al., 2017, Barker et al, 2025) or synchronize auto-oscillations of the Earth's climate (Saltzman and Verbitsky, 1993, Tziperman et al., 2006, Rial et al., 2013; Nyman and Ditlevsen, 2019; Shackleton et al., 2023). However, the orbital forcing has not been considered to play a role in the origin of the MPT.

Recently, it has been proposed (Ma et al., 2024) that the amplitude of the orbital forcing may experience a change on a million-year timescale and this may have its effect on the MPT. Verbitsky and Volobuev (2025) suggested that the orbital forcing may play an even bigger role and can also change the dynamical properties of the Earth's climate system. For example, it may change the timescale of the

vertical advection of mass and temperature in ice sheets and make their dynamics sensitive to initial values. Is ice physics unique in this sense? To answer this question, in this paper we will consider the calcifier-alkalinity (C-A) model that describes entirely different physics, focusing on the interactions between a population of calcifying organisms and ocean alkalinity (Omta et al., 2013). Previously, it has been shown that:

(a) The C-A system relaxes slowly to its asymptotic state, i.e., it has a long memory of its initial conditions (Omta et al., 2013);

(b) The asymptotic state of the orbitally forced C-A system depends on its initial conditions (Omta et al., 2016).

We will demonstrate here that the relaxation of the dominant period of the orbitally forced C-A system from its initial value to the asymptotic value can include a sharp transition similar to the MPT. We will also perform a scaling analysis of the C-A model and demonstrate that the asymptotic dominant periods are defined by a conglomerate similarity parameter combining the amplitude of the orbital forcing and the initial values. In other words, *the orbital forcing enables the dominant-period sensitivity to initial values.* We will also prove that what we call an MPT-like event in terms of the alkalinity periodicity can be translated into an MPT event in terms of the glacial rhythmicity.

2. Ocean calcifier-alkalinity model

The C-A model was first formulated by Omta et al. (2013) and focuses on the throughput of alkalinity through the World's oceans. The alkalinity is a measure for the buffering capacity of seawater that controls its capacity for carbon storage through the carbonate equilibrium (Broecker and Peng, 1982; Zeebe and Wolf-Gladrow, 2001; Williams and Follows, 2011). Alkalinity is continuously transported into the oceans as a consequence of rock weathering on the continents. When alkalinity is added to the ocean, the solubility of CO_2 increases leading to an uptake of carbon from the atmosphere into the ocean. Removal of alkalinity from the water (through incorporation of calcium carbonate into the shells of calcifying organisms and subsequent sedimentation) leads to a lower CO_2 solubility and thus outgassing of carbon from the ocean into the atmosphere. The C-A model assumes that alkalinity A (mM eq) enters the ocean at a constant rate I_0 (mM eq yr^{-1}). Alkalinity is taken up by a population of calcifying organisms C (mM eq) growing with rate constant k ((mM eq)$^{-1}$ yr^{-1}) and sedimenting out at rate M (yr^{-1}).

Altogether, the model equations are:

$$\frac{dA}{dt} = I_0 - kAC \tag{1}$$

$$\frac{dC}{dt} = kAC - MC \tag{2}$$

with t the time (yr). Since there exists observational evidence of variations in calcifier productivity correlated with Milankovitch cycles (Beaufort et al., 1997; Herbert, 1997), we include a periodic forcing term in the calcifier growth parameter k:

$$k = k_0\left(1 + \alpha cos\left(\frac{2\pi t}{T}\right)\right) \tag{3}$$

As in Omta et al. (2016) and Shackleton et al. (2023), k_0 is the average value of k, α is the non-dimensional forcing amplitude, and T (yr) is the forcing period.

Generally speaking, the alkalinity budget is also affected by the seawater carbonate saturation state. In particular, calcite preservation tends to increase with increasing carbonate ion concentration (Broecker and Peng, 1982; Archer, 1996). This carbonate compensation feedback was included in the detailed multi-box version of the calcifier-alkalinity model (Omta et al., 2013). Essentially, carbonate compensation

acted as a negative feedback that enhanced the damping of the cycles. If the periodic forcing was sufficiently strong to overcome this damping, then the model behavior was very similar to the behavior of the model without carbonate compensation (see Fig. 5 in Omta et al., 2013). Here we chose to use the simpler, more parsimonious model.

Simulations with the C-A model are performed in Julia version 1.11.2. As in Shackleton et al. (2023), we use the KenCarp58 solver (Rackauckas and Nie, 2017) with a tolerance of 10^{-16} (code is available on GitHub – https://github.com/AWO-code/VerbitskyOmta).

3. Results and Discussion

The C-A system (1) – (3) produces sawtooth-shaped cycles in alkalinity, with the alkalinity rising slowly and declining steeply. This corresponds to CO_2 decreasing slowly and increasing rapidly, consistent with the ice-core record (Lüthi et al., 2008). In Fig. 1, a simulation with initial conditions $A(0) = 2.0$ mM eq, $C(0) = 4 * 10^{-5}$ mM eq, forcing strength α = 0.012, forcing period T = 40 kyr (the obliquity period, i.e., year-average insolation), and reference values for other parameters (Omta et al., 2016) is shown.

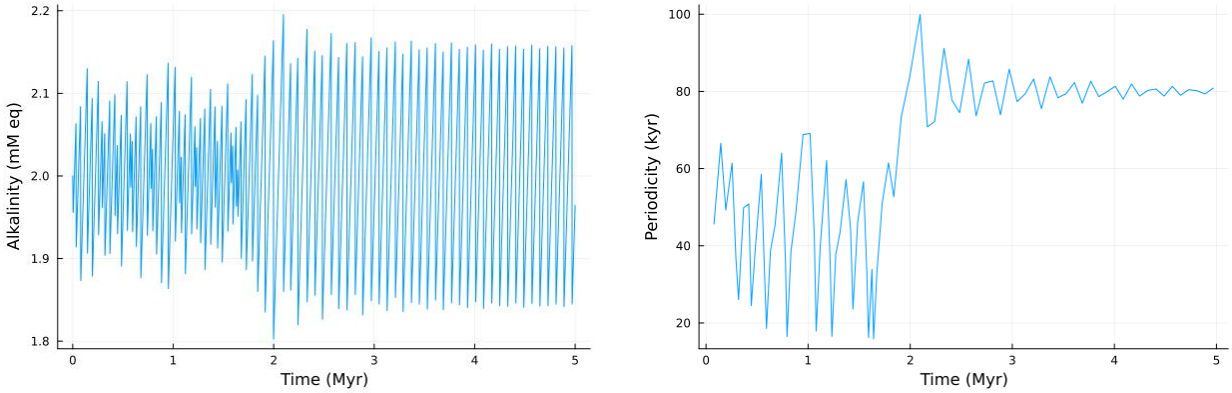

(a) (b)

Figure 1. C-A system under orbital forcing ($A(0) = 2.0$ mM eq, $C(0) = 4 * 10^{-5}$ mM eq, α = 0.012, T = 40 kyr): (a) alkalinity, (b) dominant period as a function of time

The dominant period initially evolves around the forcing period of 40 kyr, then sharply (MPT-like) increases to about 80 kyr (twice the forcing period) and stabilizes at this level. This period shift occurs through a different mechanism than in earlier studies using the C-A model, where period shifts involved noise (Omta et al., 2016) or a positive feedback (Shackleton et al., 2023) to "kick" the system from one dominant period to another one. Here no such kick is imposed: the period shift rather emerges as part of the transient dynamics of the system, as it relaxes from its initial towards its asymptotic state. For the first ~1.7 Myr of the simulation, there appears to be an approximate but not exact frequency lock, from which the system has difficulty escaping. Once the system is out of this approximate frequency lock, its period increases relatively rapidly until it reaches another multiple of the forcing period where the system becomes locked again.

In the following, we analyze how the ***initial*** and ***asymptotic*** periods may depend on the system parameters. In particular, we formulate a scaling law (Section 3.1) that we then investigate in more details through simulations (Section 3.2). In Section 3.3 we project the discovered alkalinity dynamics onto the glacial rhythmicity.

3.1 Scaling law

The C-A system of equations (1) – (3) contains seven governing parameters, including the initial conditions. Both the mean initial and the asymptotic periods have to be functions of these seven parameters. Thus, we can write:

$$P = \varphi(I_0, k_0, \alpha, T, M, A(0), C(0)) \quad (4)$$

with P the asymptotic period. If we take I_0, k_0 as parameters with independent dimensions, then according to the π-theorem (Buckingham, 1914):

$$\frac{P}{\tau} = \Phi\left[\alpha, \frac{T}{\tau}, M\tau, \frac{A(0)}{F}, \frac{C(0)}{F}\right] \quad (5)$$

Here $\tau = (k_0 I_0)^{-1/2}, F = \left(\frac{I_0}{k_0}\right)^{1/2}$.

In this study, we will focus just on two similarity parameters $\alpha, \frac{A(0)}{F}$ leaving $\frac{T}{\tau}, M\tau, \frac{C(0)}{F}$ to remain constant:

$$\frac{P}{\tau} = \Phi\left[\alpha, \frac{A(0)}{F}\right] \quad (6)$$

Using similar reasoning, we can write for the initial period P_0:

$$\frac{P_0}{\tau} = \Psi\left[\alpha, \frac{A(0)}{F}\right] \quad (7)$$

3.2 Scaling law simulations

To investigate the scaling laws (6, 7), we perform a suite of 10-Myr simulations in which we vary α and $\frac{A(0)}{F}$. The average periods during the first 1 Myr (P_0) and the last 1 Myr (P) as a function of α and $\frac{A(0)}{F}$ are presented in Figs. 2a and 2b, respectively. The range in $A(0)$, which determines the vertical axis range in Fig. 2, was chosen based on the estimated total weathering input of $CaCO_3$ (Milliman et al., 1999), which could give rise to alkalinity variations of up to ~20% on ~100-kyr timescales (Omta et al., 2013). The lower and higher ends of the range are probably a bit less likely than the middle part of the range. There is no obvious constraint on α (horizontal axis in Fig. 2), which is why we varied that parameter by two orders of magnitude. In total, Fig. 2 encompasses the results of 12,798 simulations.

(a)

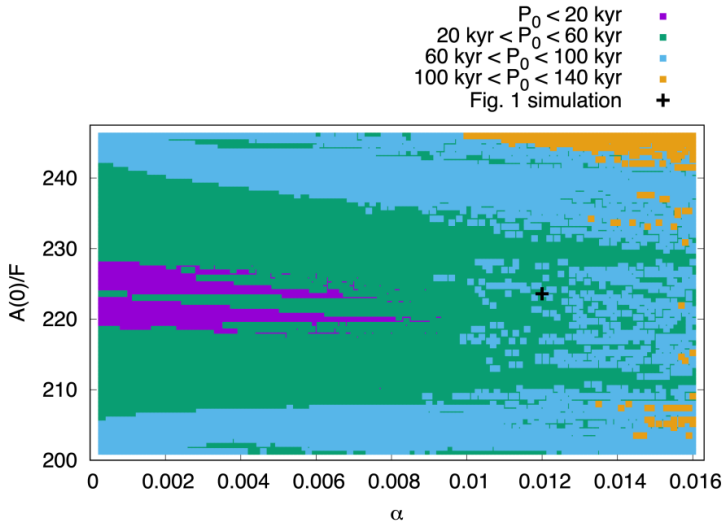

(b)

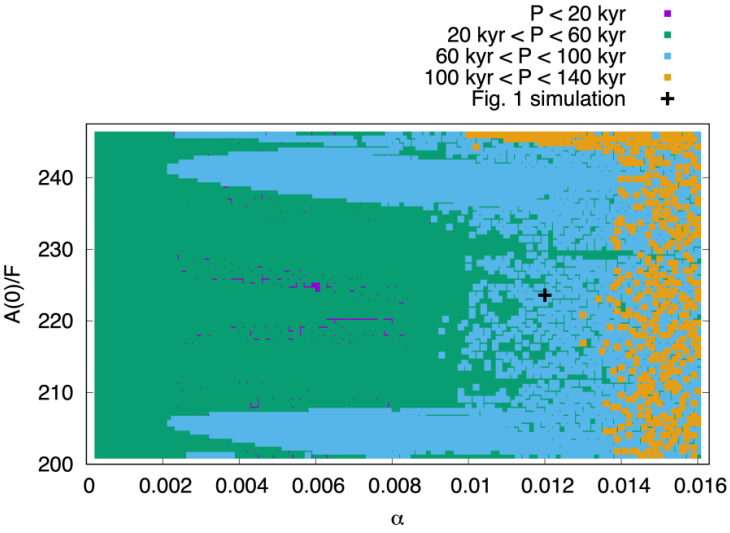

Figure 2. (a) Initial periods P_0 (average of first 1 Myr of 10-Myr simulations), and (b) asymptotic periods P (average of last 1 Myr of 10-Myr simulations). Each dot represents one simulation; the black cross indicates the parameter values for the simulation shown in Fig 1. Two similarity parameters are varied: the non-dimensional forcing strength α (horizontal axis) and the scaled initial alkalinity $\frac{A(0)}{F}$ (vertical axis). In total, Fig. 2 encompasses the results of 12,798 simulations. In all simulations, $T = 40$ kyr and $C(0) = 4 * 10^{-5}$ mM eq. Other parameters are kept constant at their reference values (Omta et al., 2016): $M = 0.1$ yr^{-1}, $k_0 = 0.05$ (mol eq)$^{-1}$ m^3 yr^{-1}, $I_0 = 4 * 10^{-6}$ mol eq m^{-3} yr^{-1}, i.e., $F = \left(\frac{I_0}{k_0}\right)^{\frac{1}{2}} = 0.00894$.

From Fig. 2, it can be observed that:

(a) P_0 and P depend on α and $\frac{A(0)}{F}$ in different manners. Most obviously, $P_0 < 20$ kyr in a significant fraction of the simulations whereas $P > 20$ kyr in almost every simulation. Furthermore, $P > 100$ kyr occurs in many more simulations than $P_0 > 100$ kyr. These differences imply that a period shift emerges in a significant fraction of the simulations.

(b) When $\alpha \to 0$, the asymptotic period P becomes independent of the initial value *A(0)* (Fig. 2b), which means that the similarity parameters $\alpha, \frac{A(0)}{F}$ in the C-A system (1) – (3) collide into one conglomerate similarity parameter $\alpha^x \left[\frac{A(0)}{F}\right]^y$ (the parameters *x* and *y* should be determined experimentally). This then provides us with the final form of the scaling law for the asymptotic period:

$$\frac{P}{\tau} = \Phi\left\{\alpha^x \left[\frac{A(0)}{F}\right]^y\right\} \tag{8}$$

The scaling law (8) implies that the *orbital forcing affects the dynamical properties of the C-A physics enabling the sensitivity of asymptotic periods to initial values*.

(c) When α increases (e.g., Gough, 1981, Ma et al., 2024), the sensitivity of the dominant asymptotic period to the initial conditions $\frac{d\left(\frac{P}{\tau}\right)}{d\left(\frac{A(0)}{F}\right)}$ also increases. Specifically, when $\alpha < 0.002$, as we have already noted, $\frac{P}{\tau}$ is not sensitive to initial values. When $0.002 < \alpha < 0.01$, it takes $\Delta\left(\frac{A(0)}{F}\right) \sim 10$ to obtain a different asymptotic period. Orbital forcing with $0.01 < \alpha < 0.014$ reduces the critical value of initial values changes to $\Delta\left(\frac{A(0)}{F}\right) \sim 1$, and finally for $\alpha > 0.014$ changes as small as $\Delta\left(\frac{A(0)}{F}\right) \sim 0.1$ lead to different asymptotic periods.

(d) Depending on $\alpha^x \left[\frac{A(0)}{F}\right]^y$, the periodicity transition could have been not just of the 40 – 80 kyr type (as shown in Fig. 1), but also of a 20 – 40, 40 – 120, or even 80 – 40 kyr type (Fig. 3).

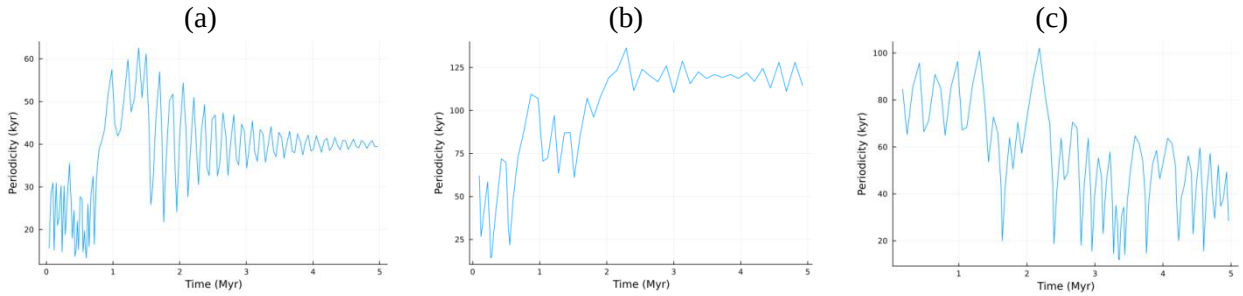

Figure 3. Alkalinity dominant-period transitions of 20 – 40 kyr (a), 40 – 120 kyr (b), and 80 – 40 kyr (c).

Most of the simulations reach their asymptotic periods within the first 1 Myr. A period shift after 1 Myr occurs in 3,217 out of the 12,798 simulations (about 25%) represented in Fig. 2. However, it is impossible to infer from the proxy data how common or rare a shift in the dominant period of the glacial-interglacial cycles actually is in the real World, since the observed Pleistocene climate is essentially a single time series.

Classical phase locking (e.g., Tziperman et al., 2006) requires some kind of dissipation in the dynamical system that erases the memory of its initial values. Obviously, this is not the case with the dominant-period trajectories we observe in Figs. 1, 2, and 3. At the same time, the asymptotic periods are multiples of the forcing period. We therefore suggest calling this phenomenon a *delayed* phase locking.

3.3 Translating alkalinity dynamics into glacial rhythmicity

To investigate the link between the modelled relaxation process and the climate system, we applied some alkalinity time series to the Verbitsky et al. (2018) model as additional forcings for the ice mass balance. This model has been derived from the scaled mass-, momentum-, and heat-conservation equations of non-Newtonian ice flow combined with an energy-balance model of global climate. In our experiments, all reference parameters of the Verbitsky et al. (2018) model remain the same, except one parameter that affects the intensity of positive feedbacks. On its own accord, the Verbitsky et al. (2018) model can produce a period shift if a positive feedback is sufficiently strong. We now set this positive feedback weaker to deprive the Verbitsky et al. (2018) model of this ability to produce MPT-like events.

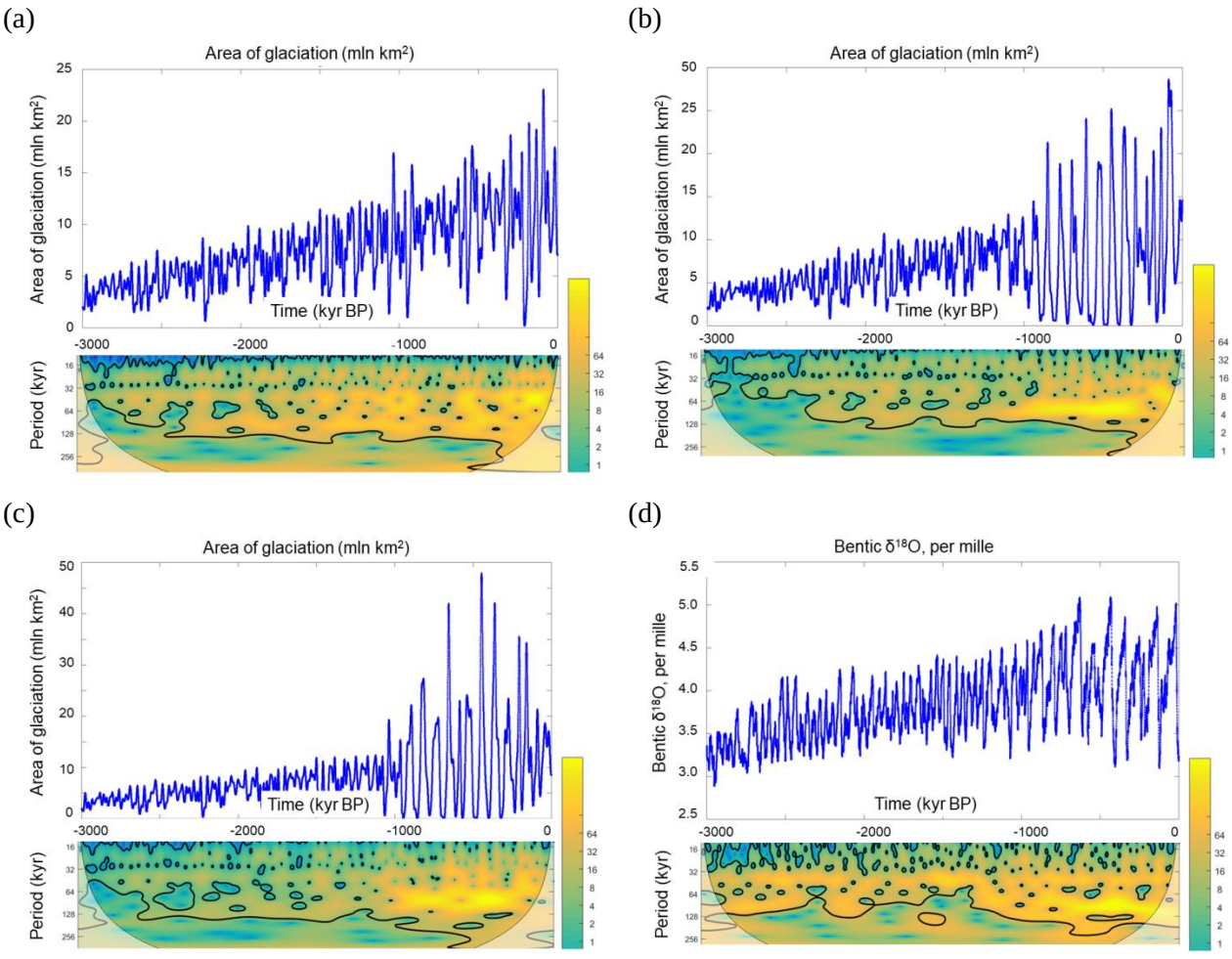

Figure 4. Ice–climate system (Verbitsky et al., 2018) response to a pure orbital (a) and to a combination of orbital and alkalinity (CO_2) forcing (b - additional alkalinity (CO_2) forcing contains a periodicity transition from 41 kyr to 80 kyr, c - additional alkalinity (CO_2) forcing contains a periodicity transition from 20 kyr to 42 kyr) presented as time series and evolutions of wavelet spectra over 3 Myr for calculated ice-sheet glaciation area (10^6 km^2) (a, b, c) and for the Lisiecki and Raymo (2005) benthic $\delta^{18}O$ record (d). The vertical axis of wavelet spectra is the period (kyr); the horizontal axis is time (kyr before present).The color scale shows the continuous Morlet wavelet amplitude, the thick line indicates the peaks with 95 % confidence, and the shaded area indicates the cone of influence for the wavelet transform.

In Figure 4a, we show the weak-positive-feedback area-of-glaciation evolution under the imposed cooling trend without additional alkalinity (CO_2) forcing. This time series does not exhibit MPT-like periodicity changes. When an additional alkalinity (CO_2) forcing containing a period shift from 41 kyr to 80 kyr is applied, the glaciation-climate system produces a 40-to-100 kyr glacial rhythmicity transition resembling the LR04 data (Figure 4b *vs* 4d). This is the case of the direct alkalinity-forced period transition that could probably be anticipated. Yet, it is quite remarkable and very unintuitive that the alkalinity forcing may entertain a more subtle interplay with the direct orbital forcing. This becomes evident in the experiment when we forced the Verbitsky et al. (2018) model with an alkalinity (CO_2) forcing containing periodicity transitions from 20 kyr to 42 kyr. A non-linear interplay of the direct orbital forcing (i.e., mid-July insolation at 65^0N, Berger and Loutre, 1991) and of ~40-kyr periods of the alkalinity forcing may produce glaciation periods of ~100 kyr also consistent with the LR04 data (Figure 4c *vs* 4d).

In this paper, we do not aspire to precisely reproduce the empirical time series and by doing so to claim any specific attribution. However, with the above experiments, we demonstrate that the calcifier-alkalinity dynamics may have a profound effect on the climate system, and what we call an MPT-like event in terms of the alkalinity periods can be translated into an MPT event in terms of glacial rhythmicity.

Generally speaking, it would be indeed interesting to explore possible interactions of different initial-value-sensitive systems such as the glaciation-climate system (Verbitsky and Volobuev, 2025), the calcifier-alkalinity system (this presentation), or, possibly, carbon cycle system (Carrillo et al., 2025). Since the MPT was a global, almost synchronous, event, the discovering of the synchronization mechanism may be an important next step. In our experiments, presented in Fig. 4, the alkalinity (CO_2), together with the direct orbital forcing, acted as the external synchronizing force for the glaciation-climate system, but many other scenarios are, indeed, possible.

4. Conclusions

The history of climate has been given to us as a single time series. For many years, perhaps somewhat naively, significant efforts have been applied to reproduce this time-series under a unique combination of the governing parameters and thus presumably to explain the history. The fundamental fact that the dominant-period trajectory is governed by a conglomerate similarity parameter $\alpha^x \left[\frac{A(0)}{F}\right]^y$ (demonstrating a property of incomplete similarity as defined by Barenblatt, 2003) tells us that the MPT could have been produced under very different combinations of the intensity of orbital forcing and initial values. Furthermore, the scaling laws (7) and (8), as they are presented in Fig. 2, show that not only periodicity transitions of the 40 – 80 kyr type (as we observe in the available data), but also of 20 – 40, 40 – 120, or even 80 – 40 kyr types would be possible. Some of these transitions, i.e., 40 – 80, 40 – 120, and, remarkably, 20 – 40 kyr types, produce glaciation MPT events consistently with the data. Most intriguingly, the conglomerate similarity parameter $\alpha^x \left[\frac{A(0)}{F}\right]^y$ implies that such an "intimate" terrestrial property as the sensitivity of alkalinity-calcination system to initial values manifests itself only under orbital forcing, and thus *the MPT exhibits a remarkable physical phenomenon of orbitally enabled sensitivity to initial values.*

We focused our paper on the past, MPT, event. Nevertheless, since we force our model with a generic obliquity, 40-kyr, forcing without a particular connection to the celestial time, any time series out of 12,798 simulations can be assumed as starting at present, and any observed periodicity transition can be considered not just as possible past transition but as potential future transition as well. Therefore, the complexity of Fig. 2 demonstrates not just the empirical data disambiguation challenge, but also the difficulty of the future climate prediction.

In this paper, when we establish a consistency between model results and empirical data, we are talking about periodicity transitions only, leaving purposely amplitude-periodicity relationship outside the

scope. Verbitsky and Crucifix (2020) demonstrated that in the short-memory ice-climate system, independent on initial values, the relationship between the glacial area amplitude S' and duration of glacial cycles P is governed by a property of scale invariance, such that $S' \sim P^2$. For the calcifier-alkalinity system, which has a long memory and dependence on the initial values, there exists a linear relationship between the amplitude and the period of the cycles. As was explained in Omta et al. (2016), this property emerges because a longer duration of the slow linear increase in alkalinity (determined by the constant term I_0 in equation (1)) implies proportionately larger amplitude of the cycle and vice versa. In the future, it will be highly desirable to compare predictions from different models regarding the periodicity and amplitude of variations in ice volume and global mean surface temperature against the newly available sea-level and global mean surface temperature data (Clark et al, 2025).

Competing interests: The authors declare that they have no conflict of interest.

Code availability. Simulations with the C-A model are performed in Julia version 1.11.2 using the KenCarp58 solver (Rackauckas and Nie, 2017) with a tolerance of 10^{-16} (https://github.com/AWO-code/VerbitskyOmta).

Data availability. This paper refers exclusively to published research articles and their data. We refer the reader to the cited literature for access to the data.

Author contributions: MYV conceived the research, AWO performed the simulations and discovered the MPT-like periodicity relaxation, MYV performed the scaling analysis and discovered the orbitally enabled sensitivity to initial values. The authors jointly wrote and edited the paper.

Acknowledgements: We are grateful to our three anonymous reviewers for their insightful reviews.

References

Abe-Ouchi, A., Saito, F., Kawamura, K., Raymo, M. E., Okuno, J., Takahashi, K., and Blatter, H.: Insolation-driven 100,000-year glacial cycles and hysteresis of ice-sheet volume, Nature, 500, 190–193, https://doi.org/10.1038/nature12374, 2013.

Archer, D. E.: An atlas of the distribution of calcium carbonate in sediments of the deep sea, Global Biogeochem. Cycles, 10, 159–174, 1996.

Ashwin, P. and Ditlevsen, P. D.: The middle Pleistocene transition as a generic bifurcation on a slow manifold, Clim. Dynam., 45, 2683–2695, https://doi.org/10.1007/s00382-015-2501-9, 2015.

Barenblatt, G. I.: Scaling, Cambridge University Press, Cambridge, UK, ISBN 0 521 53394 5, 2003.

Barker, S., Lisiecki, L. E., Knorr, G., Nuber, S., & Tzedakis, P.C.: Distinct roles for precession, obliquity, and eccentricity in Pleistocene 100-kyrglacial cycles. Science, 387, eadp3491, 2025.

Beaufort, L., Lancelot, Y., Camberlin, P., Cayre, O., Vincent, E., Bassinot, F., and Labeyrie, L.: Insolation cycles as a major control of Equatorial Indian Ocean primary production, Science, 278, 1451–1454, 1997.

Bintanja, R. and Van de Wal, R. S. W.: North American ice-sheet dynamics and the onset of 100,000-year glacial cycles, Nature, 454, 869–872, https://doi.org/10.1038/nature07158, 2008.

Broecker, W. S. and Peng, T. H.: Tracers in the Sea, Lamont-Doherty Geological Observatory, Palisades, NY, USA, ISBN 9780961751104, 1982.

Buckingham, E.: On physically similar systems; illustrations of the use of dimensional equations, Phys. Rev., 4, 345–376, 1914.

Carrillo, J., Mann, M.E., Marinov, I., Christiansen, S.A., Willeit, M. and Ganopolski, A.: Sensitivity of simulations of Plio–Pleistocene climate with the CLIMBER-2 Earth System Model to details of the global carbon cycle. Proceedings of the National Academy of Sciences, 122(23), p.e2427236122, 2025.

Clark, P. U. and Pollard, D.: Origin of the middle Pleistocene transition by ice sheet erosion of regolith, Paleoceanography, 13, 1–9, 1998.

Clark, P.U., Shakun, J.D., Rosenthal, Y., Pollard, D., Hostetler, S.W., Köhler, P., Bartlein, P.J., Gregory, J.M., Zhu, C., Schrag, D.P. and Liu, Z.: Global mean sea level over the past 4.5 million years. Science, 390 (6770), p.eadv8389, 2025.

Crucifix, M.: Why could ice ages be unpredictable?, Clim. Past, 9, 2253–2267, https://doi.org/10.5194/cp-9-2253-2013, 2013.

Gough, D. O.: Solar Interior Structure and Luminosity Variations. Sol. Phys. 74, 21–34, https://doi.org/10.1007/BF00151270, 1981.

Herbert, T.: A long marine history of carbon cycle modulation by orbital-climatic changes, Proc. Natl. Acad. Sci., 94, 8362–8369, 1997.

Lisiecki, L. E. and Raymo, M. E.: A Pliocene-Pleistocene stack of 57 globally distributed benthic $\delta^{18}O$ records, Paleoceanography, 20, PA1003, https://doi.org/10.1029/2004PA001071, 2005.

Lüthi, D., Le Floch, M., Bereiter, B., Blunier, T., Barnola, J. M., Siegenthaler, U., Raynaud, D., Jouzel, J., Fischer, H., Kawamura, K., and Stocker, T.F.: High-resolution carbon dioxide concentration record 650,000-800,000 years before present, Nature, 453, 379–382, https://doi.org/10.1038/nature06949, 2008.

Ma, X., Yang, M., Sun, Y., Dang, H., Ma, W., Tian, J., Jiang, Q., Liu, L., Jin, X. and Jin, Z.: The potential role of insolation in the long-term climate evolution since the early Pleistocene. Global and Planetary Change, 240, 104526, 2024.

Milliman, J. D., Troy, P. J., Balch, W. M., Adams, A. K., Li, Y. H., and Mackenzie, F. T.: Biologically mediated dissolution of calcium carbonate above the chemical lysocline?, Deep Sea Res. Part I, 46, 1653–1669, 1999.

Mitsui, T. and Aihara, K.: Dynamics between order and chaos in conceptual models of glacial cycles, Clim. Dynam., 42, 3087–3099, 2014.

Nyman, K. H. M., and Ditlevsen, P. D.: The Middle Pleistocene Transition by frequency locking and slow ramping of internal period, Clim. Dynam., 53, 3023–3038, https://doi.org/10.1007/s00382-019-04679-3, 2019.

Omta, A.W., Van Voorn, G.A.K., Rickaby, R.E.M., Follows, M.J.: On the potential role of marine calcifiers in glacial–interglacial dynamics, Global Biogeochem. Cycles, 27, 692–704, https://doi.org/10.1002/gbc.20060, 2013.

Omta, A.W., Kooi, B.W., Van Voorn, G.A.K., Rickaby, R.E.M., Follows, M.J.: Inherent characteristics of sawtooth cycles can explain different glacial periodicities, Clim. Dynam., 46, 557–569, https://doi.org/10.1007/s00382-015-2598-x, 2016.

Paillard, D.: Quaternary glaciations: from observations to theories, Quaternary Sci. Rev., 107, 11–24, https://doi.org/10.1016/j.quascirev.2014.10.002, 2015.

Peacock, S., Lane, E., and Restrepo, J. M.: A possible sequence of events for the generalized glacial-interglacial cycle, Global Biogeochem. Cycles, 20, GB2010, https://doi.org/10.1029/2005GB002448, 2006.

Pérez-Montero, S., Alvarez-Solas, J., Swierczek-Jereczek, J., Moreno-Parada, D., Robinson, A., and Montoya, M.: Understanding the Mid-Pleistocene transition with a simple physical model, EGUsphere [preprint], https://doi.org/10.5194/egusphere-2025-2467, 2025.

Rackauckas, C. and Nie, Q.: Differential equations.jl - A performant and feature-rich ecosystem for solving differential equations in Julia, J. Open Res. Softw., 5, 15, https://doi.org/10.5334/jors.151, 2017.

Raymo, M. E., Lisiecki, L. E., and Nisancioglu, K. H.: Plio-Pleistocene Ice Volume, Antarctic Climate, and the Global $\delta^{18}O$ Record, Science, 313, 492–495, https://doi.org/10.1126/science.1123296, 2006.

Rial, J. A., Oh, J., and Reischmann, E.: Synchronization of the climate system to eccentricity forcing and the 100,000-year problem, Nature Geosci., 6, 289–293, https://doi.org/10.1038/ngeo1756, 2013.

Riechers, K., Mitsui, T., Boers, N., and Ghil, M.: Orbital insolation variations, intrinsic climate variability, and Quaternary glaciations, Clim. Past, 18, 863–893, https://doi.org/10.5194/cp-18-863-2022, 2022.

Saltzman, B. and Verbitsky, M. Y.: Multiple instabilities and modes of glacial rhythmicity in the Plio-Pleistocene: a general theory of late Cenozoic climatic change, Clim. Dynam., 9, 1–15, 1993.

Scherrenberg, M. D. W., Berends, C. J., and Van de Wal, R. S. W.: CO_2 and summer insolation as drivers for the Mid-Pleistocene Transition, Clim. Past, 21, 1061–1077, https://doi.org/10.5194/cp-21-1061-2025, 2025.

Shackleton, J. D., Follows, M. J., Thomas P. J., and Omta, A. W.: The Mid-Pleistocene Transition: a delayed response to an increasing positive feedback? Clim. Dynam., 60, 4083–4098, https://doi.org/10.1007/s00382-022-06544-2, 2023.

Tzedakis, P. C., Crucifix, M., Mitsui, T., and Wolff, E. W.: A simple rule to determine which insolation cycles lead to interglacials, Nature, 542, 427–432, https://doi.org/10.1038/nature21364, 2017.

Tziperman, E., Raymo, M. E., Huybers, P., and Wunsch, C.: Consequences of pacing the Pleistocene 100 kyr ice ages by nonlinear phase locking to Milankovitch forcing, Paleoceanography, 21, PA4206, https://doi.org/10.1029/2005PA001241, 2006.

Verbitsky, M. Y. and Crucifix, M.: π-theorem generalization of the ice-age theory, Earth Syst. Dynam., 11, 281–289, https://doi.org/10.5194/esd-11-281-2020, 2020.

Verbitsky, M. Y. and Crucifix, M.: ESD Ideas: The Peclet number is a cornerstone of the orbital and millennial Pleistocene variability, Earth Syst. Dynam., 12, 63–67, https://doi.org/10.5194/esd-12-63-2021, 2021.

Verbitsky, M. Y. and Volobuev, D.: Milankovitch theory "as an initial value problem": Implications of the long memory of ice advection, Earth Syst. Dynam., 16, 1989–2002, https://doi.org/10.5194/esd-16-1989-2025, 2025.

Verbitsky, M. Y., Crucifix, M., and Volobuev, D. M.: A theory of Pleistocene glacial rhythmicity, Earth Syst. Dynam., 9, 1025–1043, https://doi.org/10.5194/esd-9-1025-2018, 2018.

Willeit, M., Ganopolski, A., Calov, A., and Brovkin, V.: Mid-Pleistocene transition in glacial cycles explained by declining CO_2 and regolith removal, Science Advances 5, 4, https://www.science.org/doi/10.1126/sciadv.aav7337, 2019.

Williams, R.G. and Follows, M.J.: Ocean dynamics and the carbon cycle, Cambridge University Press, Cambridge, UK, ISBN 9780521843690, 2011.

Zeebe, R. E. and Wolf-Gladrow, D.A.: CO_2 in seawater: Equilibrium, kinetics, isotopes, Elsevier, Amsterdam, Netherlands, ISBN 9780444509468, 2001.